This article has been accepted for publication in a future issue of this journal, but has not been fully edited. Content may change prior to final publication. Citation information: DOI 10.1109/ACCESS.2021.3109465, IEEE Access

Date of publication xxxx 00, 0000, date of current version xxxx 00, 0000.

Digital Object Identifier 10.1109/ACCESS.2017.DOI

A hardware-in-the-loop Water Distribution Testbed dataset for cyber-physical security testing

L. FARAMONDI[1], F. FLAMMINI[2] (Senior Member, IEEE), S. GUARINO[1], and R. SETOLA[1] (Senior Member, IEEE)

[1]Unit of Automatic Control, University Campus Bio-Medico di Roma, Via Alvaro del Portillo 21, 00128, Rome, Italy
[2]School of Innovation, Design and Engineering, Mälardalen University, Hamngatan 15, 63220, Eskilstuna, Sweden

Corresponding author: S. Guarino (e-mail: s.guarino@unicampus.it).

ABSTRACT This paper presents a dataset to support researchers in the validation process of solutions such as Intrusion Detection Systems (IDS) based on artificial intelligence and machine learning techniques for the detection and categorization of threats in Cyber Physical Systems (CPS). To this end, data have been acquired from a hardware-in-the-loop Water Distribution Testbed (WDT) which emulates water flowing between eight tanks via solenoid-valves, pumps, pressure and flow sensors. The testbed is composed of a real subsystem which is virtually connected to a simulated one. The proposed dataset encompasses both physical and network data in order to highlight the consequences of attacks in the physical process as well as in network traffic behaviour. Simulations data are organized in four different acquisitions for a total duration of 2 hours by considering normal scenario and multiple anomalies due to cyber and physical attacks.

INDEX TERMS artificial intelligence, cyber-physical systems, dataset, intrusion detection, machine learning, water distribution, security, testbed, threat recognition

I. INTRODUCTION

INDUSTRIAL Control Systems (ICS) are composed of physical and cyber components used to control industrial processes such as in the case of manufacturing, production, and distribution scenarios [1]. Those key elements are also known as Cyber-Physical Systems (CPS), which enable the connection between the operations of the industrial physical plant and the computing and communication infrastructure [2]. They have a crucial role in an ICS because they define both the correct behaviour of the physical process and the correct communication with the Supervisory Control and Data Acquisition (SCADA) systems. CPSs are widely employed in different fields such as smart grids [3] [4], oil and natural gas pipelines [5] and water treatment [6]. Because of their critical role, physical faults, such as broken valves or pumps and cyber attacks can lead to dangerous consequences which can vary from simple modifications of network traffic behaviour, such as scanning attacks, to catastrophic events such as loss of service and kinetic effects with dangerous consequences in terms of injury to people, environmental pollution, and physical damage to equipment [4].

In particular, during the last years, cyber-security has become a critical concern in ICSs due to the widespread usage of wireless networks as well as the opening of industrial networks to the Internet. Despite the benefits of such strategies, such as remote maintenance, simpler adjustment of machines and a constant flow of information, the number of attacks against ICS networks has significantly increased, as reported by Kaspersky in its ICS-CERT annual report [7].

For these reasons, different types of testbeds are needed to measure the effects of cyber and physical attacks on industrial processes and to assess security countermeasures, as witnessed by the results reported in recent scientific literature [8], [9], [10].

Among the most widespread solutions to secure CPSs, we can mention Intrusion Detection Systems (IDS) and Intrusion Prevention Systems (IPS) [13], for network monitoring (NIDS) and host monitoring (HIDS). In particular, recent scientific literature is addressing areas such as artificial intelligence and machine learning for IDSs and IPSs [14], [15], which seem to be particularly effective in recognizing unforeseen attacks [16], [17], [18]. A crucial point is the evaluation of these systems in order to assess their ability to detect attacks: to that aim, realistic and sufficiently complex datasets are necessary.

Scientific literature provides some datasets such as KDD-

Dataset	Network data			Physical data		
	Available	N° of samples	N° of features	Available	N° of samples	N° of features
[11]	X	X	X	✓	66.893	7
[12]	✓	∼ 400 M	18	✓	∼ 1 M	51
Our solution	✓	∼ 20 M	15	✓	9206	41

	Attack types				Testbed			
	DoS attack	MITM attack	Scanning attack	Physical attacks	N° of PLC	N° of sensors	N° of tanks	N° of actuators
[11]	✓	✓	X	✓	1	5	2	2
[12]	X	✓	X	X	6	24	3	27
Our solution	✓	✓	✓	✓	4	12	8	28

TABLE 1: Datasets comparison in terms of network data, physical data, attack types and testbed structure

99 [19] with its updated version NSL-KDD99 [20], UNSW-NB15 [21] and CTU-13 dataset [22]; however, all of them present Information Technology (IT) network traffic without any reference to physical plants. Therefore, there is the need for new datasets with traffic taken from Operational Technology (OT) networks where hardware and software are used to monitor and control physical processes, devices and infrastructure [23]. Moreover, in addition to the network traffic, data taken from Programmable Logic Controllers (PLC) are necessary in order to inquire the effects of cyber and physical attacks against the physical plant [24].

In [11], the authors provide a CPS dataset composed of two tanks, two pumps, one ultrasound sensor, four liquid level sensors and one PLC. Data consist of PLC register values which are reported in 15 `csv` different files. Each of these refers to normal traffic and different types of attacks both physical, such as a person hitting a tank and cyber such as Denial of Service (DoS). The excessive simplicity and the lack of network traffic make this dataset insufficient to guarantee a realistic evaluation of IDSs or IPSs.

On the other hand, the dataset described in [12] is more complex and sophisticated: it is provided by iTrust, the Centre for Research in Cyber Security at the Singapore University. The dataset refers to a Secure Water Treatment (SWAT) testbed consisting of six different stages each of which characterized by a particular physical process controlled by one PLC. Data are reported in `csv` files: one refers to the physical variables read from PLCs while other 784 files report MODBUS-only network traffic. Attacks are launched against the physical elements such as pumps or valves or against the communication network between sensors, actuators and PLCs in order to corrupt exchanged information. Thus, there is no reference to different types of cyber attack such as DoS and scanning attacks which are typically launched against ICS networks, as described in [25] and in [26]. Moreover, the authors do not consider attacks against the communication network between the SCADA, which acquires the data, and the PLCs. Another possible issue of this dataset is the size; specifically, authors provide about 1 million samples for the physical dataset and a total of about 400 million samples for the network one. This characteristic leads researchers to adopt small and random subsets of the dataset causing serious difficulty in comparing results of different research works, as happened in [27] and explained in [20].

This paper aims to overcome these limitations by providing a hardware-in-the-loop cyber-physical dataset obtained from a Water Distribution Testbed (WDT) [28]. The testbed is partially simulated thanks to the *minicps* tool in order to represent a more complex scenario by increasing the number of tanks and PLCs connected to the ICS network [29]. Data are both physical measurements taken from PLCs and network traffic presenting normal and malicious packets under different types of attacks. Moreover, the limited number of samples makes it affordable to test different IDS solutions on the complete set without the need to select a small random partition. In fact, even if the complexity of a dataset is important in order to faithfully emulate a real industrial plant, a too large dataset is not properly managed by machine learning algorithms reducing its usability [30]. Thus, evaluation results of different papers could be effectively compared in order to identify the best algorithms without any influence from the selected random data partitions.

Therefore, the main contributions are as follows:

- An ICS dataset which provides both physical and network data in order to highlight the relations between cyber and physical aspects of the system.
- A balanced complex dataset which can provide a higher number of cyber and physical attack types and more realistic scenarios by keeping, at the same time, a small number of samples. In this way, we provide a reduced sized dataset which ensures a good trade-off between complexity and usability.

Table 1 summarizes the key features of our dataset in relation to those described in [11] and [12].

The remainder of the paper is organised as follows. Section 2 describes the water distribution testbed and network topology. Section 3 describes the data acquisition and the attacks launched against the testbed. Section 4 describes the organization of the dataset. Section 5 provides some preliminary results by applying four machine learning algorithms; while Section 6 concludes the paper.

II. WATER DISTRIBUTION TESTBED

A. PHYSICAL CHARACTERISTICS

The WDT is composed of two main subsystems: a real one and a simulated one. As illustrated in Figure 1, the real subsystem consists of 5 tanks ($T_1^r \ldots T_5^r$), 20 solenoid valves ($V_1^r \ldots V_{20}^r$), 4 pumps ($P_1^r \ldots P_4^r$) and 5 pressure sensors ($S_1^r \ldots S_5^r$) under each tank. In addition, 8 manual valves are provided in order to simulate water leaks from tanks or pipes. Specifically, tanks are made of polyurethane and are characterized by the following dimensions:

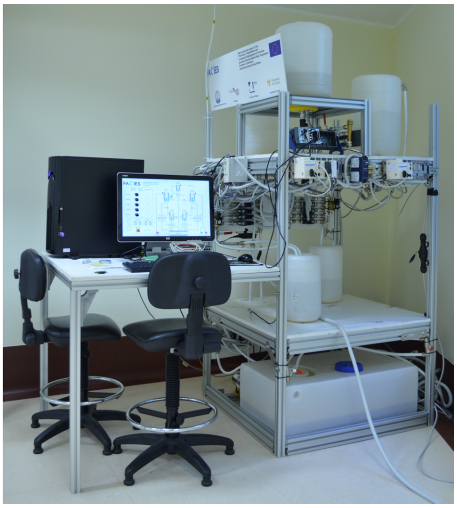

FIGURE 1: Real subsystem of the WDT

- S_3^r and S_4^r: height = $36cm$, circumference = $70cm$
- S_1^r and S_2^r: height = $45cm$, circumference = $90cm$
- S_5^r: height = $40cm$, circumference = $100cm$

Solenoid valves are Evian©Series 263-Model D263DVP powered at 24V. Each tank has a multiple number of outlet valves in order to modulate the output flow. Specifically, as shown in Figure 2, T_1^r is equipped with outlet valves V_1^r, V_2^r, V_3^r and V_4^r; T_2^r with V_5^r, V_6^r, V_7^r and V_8^r; T_3^r with V_{10}^r, V_{11}^r and V_{12}^r; T_4^r with V_{13}^r, V_{14}^r and V_{15}^r and T_5^r with V_{19}^r and V_{20}^r. Pressure sensors are WIKA©S-11, with a measurement range of 0 . . . 0.1 bar.

Pumps P_1^r, P_2^r and P_3^r are Mini-Type Pipe Pump 151410 with a maximum flow of $20l/min$ while P_4^r is a EK-DCP 2.2 with a maximum flow of $6l/min$.

Tanks are connected by pipes in cross-linked multi-layer polyurethane (PE-Xb) with an external diameter of 7/8″.

The simulated subsystem has been implemented by using the *minicps* tool, a lightweight simulator for accurate network traffic in industrial control systems, with basic support for physical layer interaction. It was installed in an Ubuntu machine with the following characteristics: Intel® Xeon® CPU E5-2620 v2 @ 2.10 GHz with a RAM of 16 GB. As illustrated in Figure 2, the simulated environment adds complexity to the real testbed with the addition of 3 tanks ($T_6^s \dots T_8^s$), 2 pumps (P_5^s, P_6^s), 4 flow sensors ($F_1^s \dots F_4^s$), 2 solenoid valves (V_{21}^s, V_{22}^s) and 3 pressure sensors ($S_6^s \dots S_8^s$) for each tank. Specifically, tanks are modelled with a circumference of $100cm$ and a height of $40cm$. Pipes are modeled with an external diameter of 7/8″ while pumps are characterized by a flow of $4l/min$.

The two subsystems form a water distribution testbed in a hardware-in-the-loop fashion where water flow goes from the real subsystem to the simulated one and vice versa.

B. PROCESS DETAILS

For the sake of clarity, we now describe the details about the nominal behaviour of the process. According to the scheme represented in Figure 3, the process consists of four stages each of which is controlled by a specific PLC. The first stage $S1$, which is controlled by the real PLC, PLC_1^r, begins by pumping the water from the reservoir towards two different paths:

- **Path 1**: The water is pumped by P_1^r towards T_2^r. Then, thanks to V_{17}^r, it starts to fill up T_3^r. When the water level reaches a specific threshold, V_{10}^r, V_{11}^r and V_{12}^r are activated in order to get water back to the reservoir.
- **Path 2**: The water is pumped by P_2^r towards T_1^r. Then, P_4^r is activated in order to fill up T_5^r. When the water level reaches a specific threshold, P_4^r is deactivated. As a result, the remaining water in T_1^r is drained towards T_4^r thanks to the opening of V_{18}^r and then through valves V_{13}^r, V_{14}^r and V_{15}^r towards the reservoir.

The second stage $S2$ starts when water level in T_5^r reaches the predefined threshold. PLC_2^s, simulated in *minicps*, opens solenoid valve V_{20}^r and starts to fill up T_6^s: its water level increases as much as water level in T_5^r decreases. Thus, even if V_{20}^r drains the water towards the reservoir, it is virtually deviated towards T_6^s in order to start the simulated physical process in *minicps*. The water then reaches stage $S3$ thanks to P_5^s controlled by PLC_3^s: T_7^s starts to fill up while F_1^s records water flow downstream of the pump.

The last stage $S4$ is controlled by PLC_4^s which defines water flowing from T_7^s towards T_8^s thanks to P_6^s. Also in this case the water flow is measured by F_2^s. When the water level in T_8^s reaches a specific threshold, PLC_4^s opens solenoid valve V_{22}^s in order to drain virtually the water towards the reservoir.

C. NETWORK ARCHITECTURE

Network architecture is consistent with the typical three-layer SCADA architecture defined in [31] and shown in Figure 4. The adopted communication protocol is MODBUS TCP/IP which is the de-facto standard used in industrial networks [32].

The first layer is the Field Instrumentation Control Layer which consists of sensors and actuators connected to the PLCs via wired links. All of them are connected to the I/O analog or digital module of the PLCs with the exception of flow sensors F_1^s and F_2^s which are MODBUS TCP/IP sensors with their own IP addresses.

The second layer is the Process Control Layer which consists of the four PLCs. In particular, the real one is a Modicon M340 equipped with BMX P342020 processors, DDM16025 discrete I/O and AMM0600 mixed analog I/O modules.

The third and last layer is the Process Control Layer which consists of the Supervisory Control and Data Acquisition system Movicon 11.6 installed in a Windows Server 2012 machine with the following characteristics: Intel® Xeon® CPU E5-2620 v2 @ 2.10 GHz with a RAM of 16 GB. The

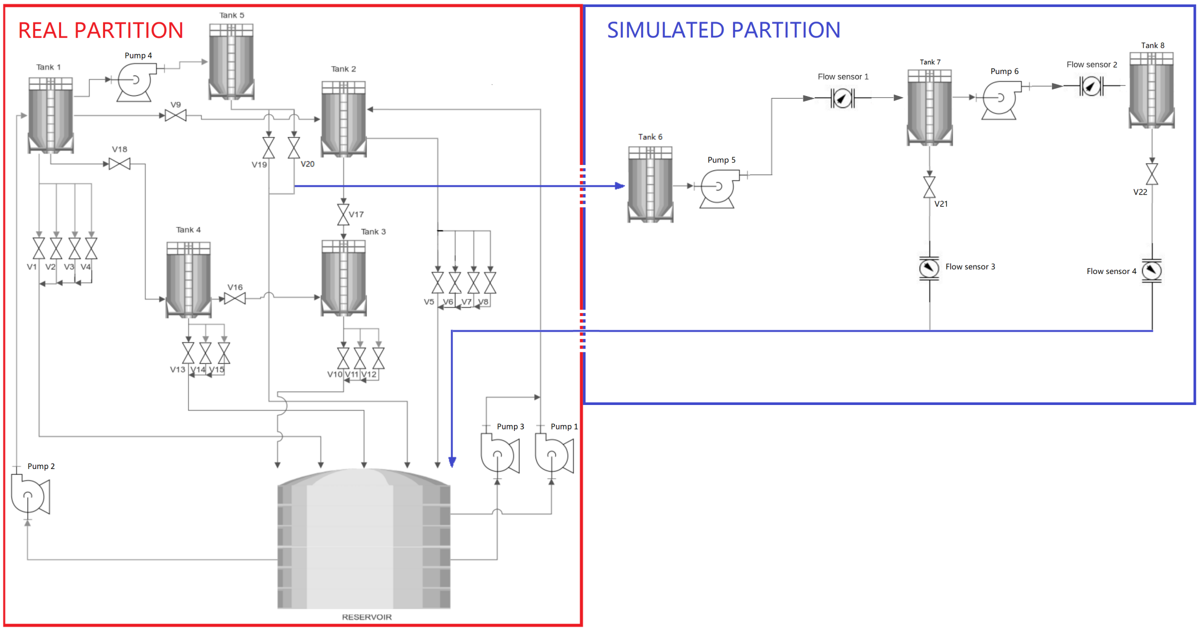

FIGURE 2: WDT schematic: the left red rectangle represents the real subsystem while the right blue rectangle the simulated subsystem of the water testbed. Blue rows represent virtual water flowing between the two subsystems.

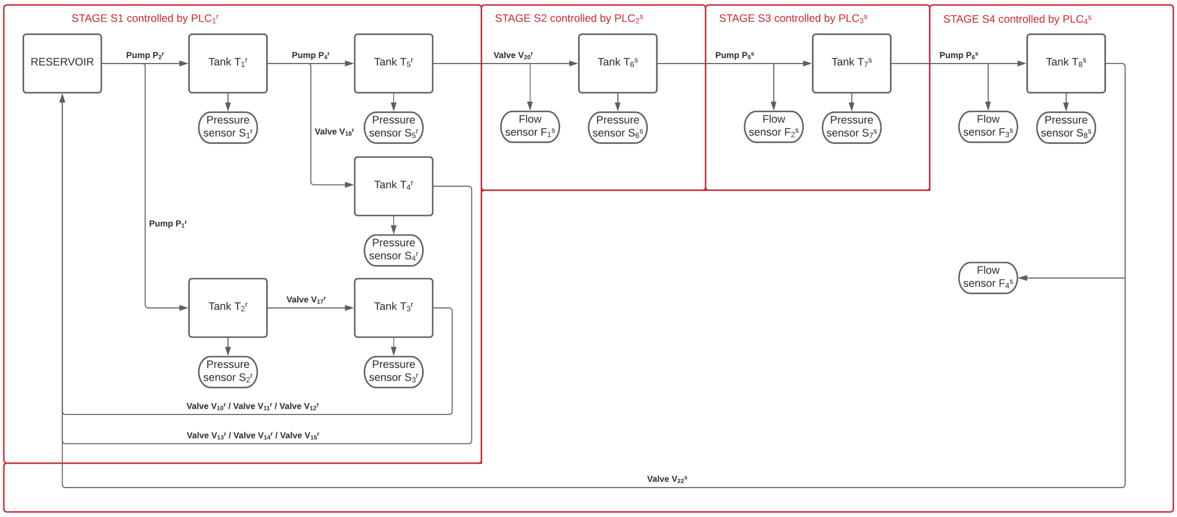

FIGURE 3: WDT physical process divided into 4 stages: the first is controlled by the real PLC, PLC_1^r, while the remaining ones are controlled by the simulated PLCs, PLC_2^s, PLC_3^s and PLC_4^s

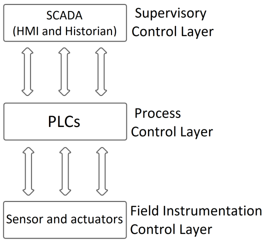

FIGURE 4: SCADA architecture

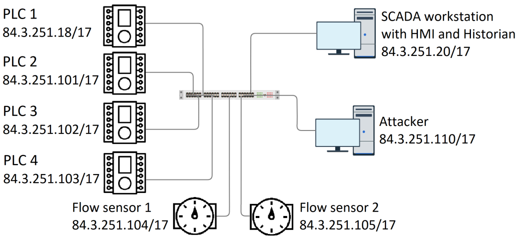

FIGURE 5: SCADA network

Type	Class	Subclass	Description
Cyber	Man-In-The-Middle (MITM) attack	ARP poisoning	Attack against MODBUS communication protocol with the intention to modify packets data payload
Cyber	Denial of Service (DoS) attack	TCP flood ICMP flood Land attack	Attack against single hosts with the intention to saturate their resources and to disconnect them from the network
Cyber	Scanning attack	SYN scan FIN scan Null scan XMAS scan	Attack against hosts with the intention to gather network information about these devices
Physical	Water leak	Opening of manual valves	Attack consisting in opening manual valves in order to generate water leaks from tanks
Physical	Sensors and pumps breakdown		Attack consisting in blocking sensors and pumps

TABLE 2: Cyber and physical attacks

First acquisition *attack_1.csv*, *phy_att_1.csv*

# scenario	Start time	End time	Type of attack	Effects on physical process	Effects on network traffic	Elapsed time	Cycle
1.1	09/04/2021 18:25:48	09/04/2021 18:28:14	*Cyber*: MITM attack against PLC_2^s and PLC_3^s. Affected sensor value: S_6^s.	✓	✓	2’20”	I
1.2	09/04/2021 18:30:08	09/04/2021 18:31:14	*Physical*: water leak from T_2^r towards T_3^r and from T_2^r towards reservoir	✓	X	1’21”	II
1.3	09/04/2021 18:34:11	09/04/2021 18:35:38	*Cyber*: MITM attack against PLC_1^r and PLC_2^s. Affected sensor value: S_5^r.	✓	✓	1’14”	III
1.4	09/04/2021 18:38:38	09/04/2021 18:39:50	*Physical*: P_2^r breakdown and water leak from T_1^r towards T_4^r	✓	X	12”	IV
1.5	09/04/2021 18:43:52	09/04/2021 18:45:54	*Cyber*: MITM attack against PLC_3^s and PLC_4^s. Affected sensor value: S_7^s.	✓	✓	5’26”	IV
1.6	09/04/2021 18:49:02	09/04/2021 18:51:18	*Physical*: water leak from T_2^r towards T_3^r	✓	X	14”	VI
1.7	09/04/2021 18:58:05	09/04/2021 18:59:32	*Cyber*: MITM attack against F_1^s and PLC_3^s. Affected sensor value: F_1^s.	✓	✓	3’59”	VII
1.8	09/04/2021 19:00:40	09/04/2021 19:02:07	*Cyber*:MITM attack against F_2^s and PLC_3^s. Affected sensor value: F_2^s.	✓	✓	1’49”	VIII

Second acquisition *attack_2.csv*, *phy_att_2.csv*

# scenario	Start time	End time	Type of attack	Effects on physical process	Effects on network traffic	Elapsed time	Cycle
2.1	19/04/2021 15:38:52	19/04/2021 15:38:52	*Cyber*: SYN scan against PLC_1^r	X	✓	1’40”	I
2.2	19/04/2021 15:40:09	19/04/2021 15:40:09	*Cyber*: FIN scan against PLC_2^s	X	✓	2’57”	I
2.3	19/04/2021 15:41:10	19/04/2021 15:41:10	*Cyber*: XMAS scan against PLC_3^s	X	✓	3’58”	I
2.4	19/04/2021 15:42:03	19/04/2021 15:42:03	*Cyber*: Null scan against PLC_4^s	X	✓	0’0”	II
2.5	19/04/2021 15:43:46	19/04/2021 15:44:22	*Cyber*: ICMP flood attack against PLC_1^r from spoofed HMI IP address	✓	✓	1’42”	II
2.6	19/04/2021 15:48:15	19/04/2021 15:48:56	*Physical*: breakdown of P_4^r	✓	X	1’2”	III
2.7	19/04/2021 15:51:16	19/04/2021 15:51:16	*Cyber*: Null scan against PLC_3^s	X	✓	4’3”	III
2.8	19/04/2021 15:54:39	19/04/2021 15:55:59	*Physical*: breakdown of V_{20}^r	✓	X	1’58”	IV
2.9	19/04/2021 15:58:40	19/04/2021 15:58:40	*Cyber*: SYN scan against PLC_1^r	X	✓	5’59”	IV
2.10	19/04/2021 15:59:57	19/04/2021 16:00:10	*Cyber*: ICMP flood against PLC_1^r	X	✓	1’12”	V
2.11	19/04/2021 16:04:39	19/04/2021 16:04:39	*Cyber*: FIN scan against PLC_2^s	X	✓	1’40”	VI
2.12	19/04/2021 16:08:26	19/04/2021 16:10:01	*Cyber*: MITM attack against PLC_3^s and PLC_4^s. Affected sensor value: S_7^s.	✓	✓	4’27”	VI
2.13	19/04/2021 16:11:46	19/04/2021 16:12:14	*Cyber*: TCP flood against PLC_1^r from spoofed PLC_2^s IP address	✓	✓	2’58”	VII

Third acquisition *attack_3.csv*, *phy_att_3.csv*

# scenario	Start time	End time	Type of attack	Effects on physical process	Effects on network traffic	Elapsed time	Cycle
3.1	09/04/2021 19:43:17	09/04/2021 19:44:08	*Physical*: breakdown of P_4^r	✓	X	1’5”	I
3.2	09/04/2021 19:45:52	09/04/2021 19:46:21	*Cyber*: ICMP flood against HMI from its spoofed IP address	X	✓	3’40”	I
3.3	09/04/2021 19:49:54	09/04/2021 19:50:48	*Physical*: breakdown of V_{20}^r	✓	X	2’1”	II
3.4	09/04/2021 19:54:00	09/04/2021 19:54:45	*Physical*: breakdown of P_2^r	✓	X	28”	III
3.5	09/04/2021 19:55:29	09/04/2021 19:56:15	*Cyber*: ICMP flood against PLC_1^r with huge payloads	✓	✓	1’58”	III
3.6	09/04/2021 19:58:02	09/04/2021 19:59:09	*Cyber*: MITM attack against PLC_3^s and PLC_4^s. Affected sensor value: S_7^s.	✓	✓	4’30”	III
3.7	09/04/2021 20:01:18	09/04/2021 20:02:03	*Cyber*: MITM attack against PLC_3^s and PLC_4^s. Affected sensor value: S_7^s.	X	✓	2’20”	IV

TABLE 3: Attack scenarios per each acquisition

SCADA includes the Human Machine Interface (HMI) and a Historian which reads and stores data from PLCs.

As shown in Figure 5, the communication network consists of four PLCs, 2 MODBUS TCP/IP flow sensors, the SCADA workstation and an additional host, a Kali Linux machine, which was used to launch cyber attacks, described in detail in Section III.

III. ATTACKS AGAINST THE TESTBED

As mentioned in Section I, in this work, we considered two different types of attack:

- **Physical attacks:** they are defined as attacks against the physical elements such as sensors and actuators. Some examples are leaks from tanks and pipes, sensors or actuators breakdown.
- **Cyber attacks:** they are defined as attacks against hosts (SCADA, PLC, and flow sensor) or communication links. Some examples are Denial of Service (DoS) attacks, scanning attacks and MITM attacks.

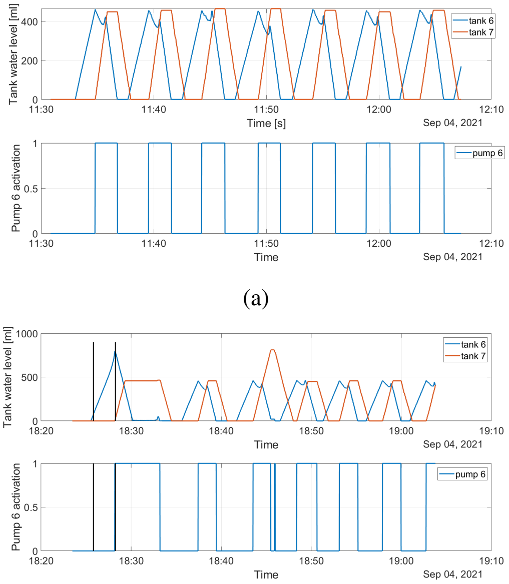

(a)

(b)

FIGURE 6: Effect of a MITM attack against PLC_2^s and PLC_3^s on physical process (Scenario 1.1). The attack changes the water level value of T_6^s requested by PLC_3^s to PLC_2^s. (a) shows the normal scenario while (b) the attack effect. Black lines indicate the start and the end of the MITM attack.

According to the ontology provided in [25] and [26], each type of attack is classified and described in Table 2. Attacks can be divided into five different classes and, for each of them, we considered specific subclasses such as SYN scan and FIN scan for scanning attacks [26]. All the attacks are launched against both real and simulated subsystems of the WDT. In particular, cyber attacks are carried out thanks to a Kali Linux machine with the following hardware configuration: Intel R, Core(TM) i7-8750H CPU @2.20GHz (1CPU), 4GB RAM.

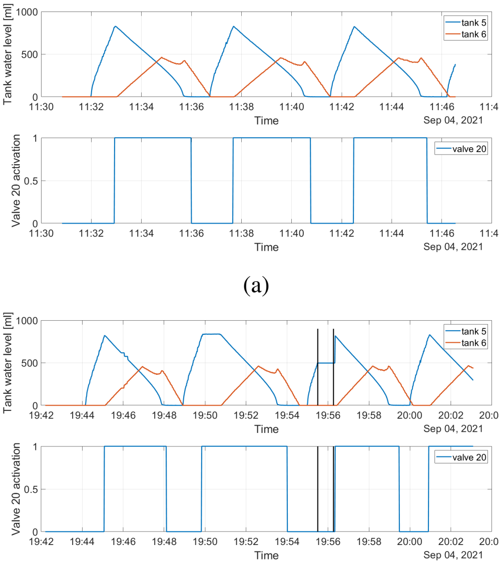

(a)

(b)

FIGURE 7: Effect of a DoS attack against PLC_1^r on physical process (Scenario 3.5). The attack causes the disconnection of PLC_1^r from the network causing a delay in the filling of T_6^s. (a) shows the normal scenario while (b) the attack effect. Black lines indicate the start and the end of the DoS attack.

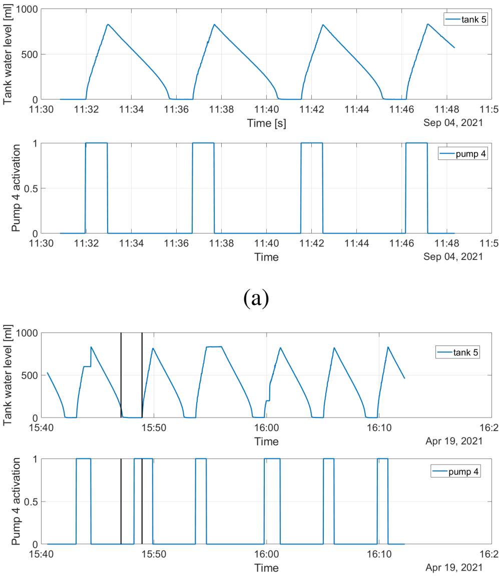

(a)

(b)

FIGURE 8: Effects of a physical attack against P_4^r on the physical process (Scenario 2.6). The attack causes the breakdown of P_4^r, which stops water flow towards T_5^r. (a) shows the normal scenario, while (b) the effect of the attack. Black lines indicate the start and the end of the physical attack.

A. ATTACK SCENARIOS

Considering the different attacks described in Table 2, we have defined 28 attack scenarios by varying the start time and the specific target. As summarized in Table 3, the effects of such attacks scenarios are collected into three of the four different acquisitions which will be described in-depth in Section IV-A. Table 3 shows the scenarios specifying if a particular attack has an impact on the physical process or on the network traffic. In particular, as we expected, physical attacks have no effect on the network traffic because they are only focused on the testbed physical components. On the other hand, all cyber attacks have effects against the network traffic but not necessarily on the physical process. This behaviour depends on three factors: the time when a specific attack is launched, the current process state, and the specific target. In this view, notice that despite Scenario 3.6 and Scenario 3.7 are characterized by the same attack type (MITM), only the first one has an impact on the physical process. Specifically, in our dataset, a MITM attack fixes the requested sensor value at the last value read by the victim before the attack. Thus, in these two scenarios, the attack fixes the water level of T_7^s at the last not impaired value requested by PLC_4^s to PLC_3^s.

The presence or absence of attack effects against both physical and network behaviour makes the classification task of machine learning algorithms more complex and challenging, as we will described in Section V-D.

Figures 6, 7 and 8 show three different attack scenarios against the physical process; specifically, they refer respectively to Scenario 1.1, Scenario 3.5 and Scenario 2.6.

Figure 6 shows the effects of a MITM attack against PLC_2^s and PLC_3^s. The attacker fixes the water level of T_6^s at the last value requested by PLC_3^s to PLC_2^s before the attack. In this way, PLC_3^s will receive always the same compromised value for the entire duration of the attack. Thus, PLC_3^s does not activate P_5^s causing an anomalous water level increase in T_6^s while T_7^s remains empty until the attack ends.

Figure 7 shows the effects of a DoS attack against PLC_1^r. The attack causes the disconnection of PLC_1^r from the network while T_5^r is still filling up. As a result, PLC_2^s is not able to read the actual value of water level in T_5^r delaying the filling of T_6^s.

Figure 8 shows the effects of a physical attack against P_4^r. The attack causes the breakdown of P_4^r which stops water flow towards T_5^r.

IV. DATASET ANALYSIS

A. DATA ACQUISITION

With the aim to reduce the total size of the dataset, we provide four different acquisitions characterised by an overall duration of about 2 hours. Each acquisition consists of a certain number of cycles of the physical process in order to guarantee a sufficient knowledge about the normal operation and to define the 28 attack scenarios described in Section III. Specifically, the first acquisition lasts 1 hour and shows a total of 12 process cycles: it refers to the WDT while working in normal conditions without any attack. On the contrary, the remaining three acquisitions, which last 60 minutes, provide respectively 8, 7 and 4 process cycles. They report data about the attacks described in Section III which cause different effects on the physical process or on the network behaviour. Such effects depend on the type of attack, the time at which the attack was launched and on the particular target. Consecutive attacks were avoided if both of them caused significant variations in the physical process or network traffic: in these cases, the time between two attacks is at least equal to that necessary to get WDT back in a safe and normal condition. As shown in Table 2, attack scenarios are distributed along the different cycles and are temporally separated in order to reduce the mutual influence. Specifically, the column *Cycle* defines the specific physical cycle which is affected by the attack scenario; while, the column *Elapsed time* defines the time elapsed since the beginning of the same cycle.

The acquisitions started with all tanks empty.

For each acquisition, we provide two different datasets: a physical one, which reports the physical measurements of sensors, solenoid valves and pumps taken from PLCs and saved by the historical data recorder (Historian), and a network one, which reports packets features about the traffic exchanged in the SCADA network.

In Figures 9 and 10, the total number of samples for network and physical datasets are reported.

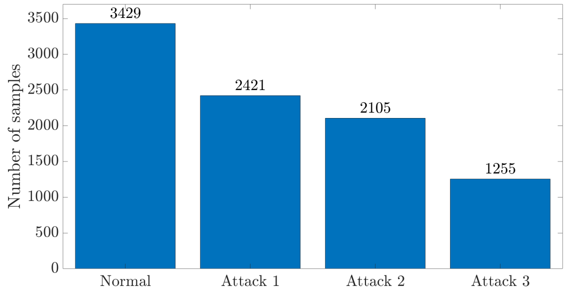

FIGURE 9: Number of samples for physical dataset reported for each acquisition

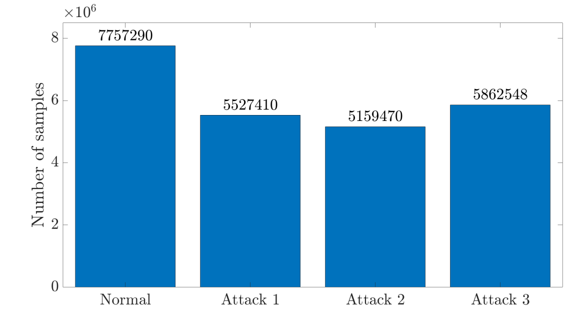

FIGURE 10: Number of samples for network dataset reported for each acquisition

B. PHYSICAL DATASET

The Historian logged the physical data every second in a `csv` file. Thus, each record represents sensors, pumps and solenoid valves states taken from the four PLCs at a particular time. Samples are defined by 41 features which are reported in Table 4.

C. NETWORK DATASET

Network traffic of all network segments was captured thanks to *Wireshark* software. Features were extracted from the outgoing `pcap` file by using *Python*. Specifically, features were selected by considering that ICS networks are more deterministic and static than IT networks where, on the contrary, changes in terms of network topology and network traffic are more frequent, as described in [33]. Taking this into account, features were selected according to [34] where the authors studied which attributes best differentiate between anomalous and normal behaviour in ICS networks. We considered packet-based features, which assist the examination of packets payload in addition to the headers. This choice is justified by the presence of attacks which affect exclusively packets payload such as the MITM attack [35], [36]. Specifically, we analyzed the effectiveness and the applicability of the following features:

- *Src IP address*: Source IP address. In ICS networks, IP addresses are assigned statically; moreover, the number of hosts is static and well-defined. Thus, the appearance of new devices has to trigger an event.
- *Dst address*: Destination IP address. As for the source, also destinations in ICS networks are fixed and well known.
- *Src MAC address*: Source MAC address. Changes in MAC to IP mapping is very infrequent. Thus, the use of ARP messages to resolve MAC addresses of unknown IP addresses has to be notified. Changes in this feature could be the consequence of malfunctions or of ARP-poisoning MITM attack.
- *Dst MAC address*: Destination MAC address. As for the source, also the destinations are well-defined. Any unknown and additional MAC address indicates the presence of malicious hosts connected to the network.
- *Src Port*: Source port. In ICS networks, ports are standard and related to the configuration of hosts and to the adopted protocols.
- *Dst Port*: Destination port. As for the source, also the destination ports are static and well-defined. Unknown ports could indicate the use of protocols which are not allowed in the specific ICS network.
- *Proto*: Protocol. Protocols in ICS networks are limited and well-defined. Thus, the appearance of new protocols has to be reported as a network modification.
- *TCP flags*. In general, TCP flags are used to indicate a specific state of a TCP connection. An attacker can vary these protocol settings in order to gather information about the networked devices such as in the case of scanning attacks.
- *Payload size*. Packets exchanged in an ICS network are well-defined and without extra buffering in order to provide real-time requirements. Thus, anomalous packet size could be the consequence of malfunctions or malicious activity.
- *MODBUS code*: MODBUS function code. In MODBUS protocol, the code specifies the type of PLC memory address which is requested. Unusual read requests have to be notified as a consequence of unauthorised PLC access.
- *MODBUS value*. Abnormal payload data could be the sign of misconfiguration or malicious actions such as MITM attacks. Changes in MODBUS values could cause a significant impact on the physical process.
- *num_pkts_src*: number of packets of the same source address in the last 2 seconds. In ICS networks, the number of connections between hosts is quite always static and constant. Any variation of this value can be the consequence of malfunctions and DoS or DDoS attacks. This feature captures an anomalous number of connections from one specific host.
- *num_pkts_dst*: number of packets of the same destination address in the last 2 seconds. This feature captures an anomalous number of connections towards one specific target.

Table 5 summarizes the list of network features we considered in our dataset. In addition to those already described, all the samples are identified by the datetime of acquisition.

D. LABELLING

To label the samples for each acquisition, we used attack logs focusing in particular on the starting time, the ending time and the type of attack. Each record is characterized by two different labels: the first one defines the type of attack while the second one is either 0 if the record is normal and 1 if the record is attack. Figure 11 shows the total number of samples divided into normal and malicious.

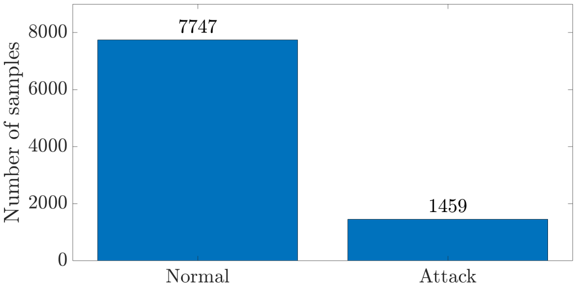

FIGURE 11: Total number of samples divided into normal and malicious

E. FINAL SHAPE OF DATASETS

We provide the two datasets in 8 different `csv` files. In particular, *attack_1*, *attack_2* and *attack_3* refer to normal

№	*Features*	*Description*	*№*	*Features*	*Description*
1	Time	Datetime of acquisition	*22*	Valv_3	State of solenoid valve 3
2	Tank_1	Pressure sensor value of tank 1	*23*	Valv_4	State of solenoid valve 4
3	Tank_2	Pressure sensor value of tank 2	*24*	Valv_5	State of solenoid valve 5
4	Tank_3	Pressure sensor value of tank 3	*25*	Valv_6	State of solenoid valve 6
5	Tank_4	Pressure sensor value of tank 4	*26*	Valv_7	State of solenoid valve 7
6	Tank_5	Pressure sensor value of tank 5	*27*	Valv_8	State of solenoid valve 8
7	Tank_6	Pressure sensor value of tank 6	*28*	Valv_9	State of solenoid valve 9
8	Tank_7	Pressure sensor value of tank 7	*29*	Valv_10	State of solenoid valve 10
9	Tank_8	Pressure sensor value of tank 8	*30*	Valv_11	State of solenoid valve 11
10	Pump_1	State of pump 1	*31*	Valv_12	State of solenoid valve 12
11	Pump_2	State of pump 2	*32*	Valv_13	State of solenoid valve 13
12	Pump_3	State of pump 3	*33*	Valv_14	State of solenoid valve 14
13	Pump_4	State of pump 4	*34*	Valv_15	State of solenoid valve 15
14	Pump_5	State of pump 5	*35*	Valv_16	State of solenoid valve 16
15	Pump_6	State of pump 6	*36*	Valv_17	State of solenoid valve 17
16	Flow_sensor_1	Flow sensor value 1	*37*	Valv_18	State of solenoid valve 18
17	Flow_sensor_2	Flow sensor value 2	*38*	Valv_19	State of solenoid valve 19
18	Flow_sensor_3	Flow sensor value 3	*39*	Valv_20	State of solenoid valve 20
19	Flow_sensor_4	Flow sensor value 4	*40*	Valv_21	State of solenoid valve 21
20	Valv_1	State of solenoid valve 1	*41*	Valv_22	State of solenoid valve 22
21	Valv_2	State of solenoid valve 2			

TABLE 4: Features of physical dataset

№	*Features*	*Description*
1	Time	Datetime of acquisition
2	Src IP address	Source IP address
3	Dst IP address	Destination IP address
4	Src MAC address	Source MAC address
5	Dst MAC address	Destination MAC address
6	Src Port	Source port
7	Dst port	Destination port
8	Proto	Protocol
9	TCP flags	CWR | ECN | URG | ACK | PSH | RST | SYN | FIN flags
10	Payload size	Size of packet payload
11	MODBUS code	MODBUS function code
12	MODBUS value	MODBUS response value
13	num_pkts_src	Number of packets of the same source address in the last 2 seconds
14	num_pkts_dst	Number of packets of the same destination address in the last 2 seconds

TABLE 5: Features of network dataset

and malicious network traffic while *phy_att_1*, *phy_att_2* and *phy_att_3* refer to the corresponding physical values of the WDT. Files *normal* and *phy_norm* refer to legitimate network and physical data.

Moreover, we provide raw network traffic packets in four *pcap* files: *attack_1.pcap*, *attack_2.pcap*, *attack_3.pcap* and *normal.pcap*).

The list of the events is defined in the file *README.xslx*.

F. USE OF THE WDT DATASET

The WDT dataset is available at the link[1] and can be used free of charge for research and study applications (non-commercial activities) as long as it is reported in the bibliography with reference to this article.

V. MACHINE LEARNING PERFORMANCE EVALUATION

As described in Section I, our dataset wants to support researchers in the validation of artificial intelligence and machine learning algorithms. In this section, we show some preliminary results by applying four different supervised machine learning algorithms to network and physical datasets.

A. CLASSIFICATION TECHNIQUES

We adopted the following machine learning algorithms: K-Nearest-Neighbor (KNN), Naïve Bayes (NB), Support Vector Machine (SVM) and Random Forest (RF).

KNN is one of the simplest classifiers [37]. It is based on the distribution of training samples in the so-called feature space; a test sample is classified with the most represented class by the k-nearest training samples.

NB is a class of probabilistic classifiers based on the Bayes' theorem which requires the strong assumption of independence between the features. It computes the a-posteriori probability of samples to belong to one of the different classes knowing the likelihood of the features [38].

SVM is one of the best classifier algorithms [39]. It computes a separating hyperplane which divides samples belonging to the two classes in the best way.

RF is an ensemble learning classifier algorithm [40]. It computes a predefined number of decision trees at training time; then it returns the most represented class by computing the mode of the classes for each individual tree.

B. EVALUATION SETUP

Considering both network and physical data, samples from all four acquisitions were joined in order to obtain only two

[1] https://ieee-dataport.org/open-access/hardware-loop-water-distribution-testbed-wdt-dataset-cyber-physical-security-testing

Algorithm	Performance metric	Physical dataset	Network dataset
KNN	Accuracy	0.98	0.77
	Recall	0.95	0.44
	Precision	0.95	0.68
	F1 score	0.95	0.53
RF	Accuracy	0.99	0.75
	Recall	0.98	0.53
	Precision	0.95	0.56
	F1 score	0.97	0.54
SVM	Accuracy	0.93	0.69
	Recall	0.92	0.99
	Precision	0.64	0.10
	F1 score	0.75	0.20
NB	Accuracy	0.93	0.75
	Recall	0.92	0.15
	Precision	0.66	0.90
	F1 score	0.77	0.27

TABLE 6: Machine learning evaluation results

different datasets: one for network traffic and one for PLC data.

Before applying machine learning classifiers, we proceeded with the standardization and the removal of identical records. Specifically, we scaled all features by removing the mean and the variance in order to make data normally distributed. Then, we removed identical records in order to reduce possible biases towards the more representative classes. Datasets were divided into training and test sets using a K-Folds cross-validation. Feature standardization was performed on training set and, subsequently, the mean and variance of training data were used to normalize the test set.

Hyperparameters of classifiers were set as follows: k=10 for the KNN and 100 trees for RF. SVM was applied with a Radial basis function kernel and, for Naïve Bayes, the Gaussian version was used.

In order to implement KNN, RF, SVM and NB, we used the Python *Scikit-learn* library [41].

C. PERFORMANCE METRICS

Performance of machine learning algorithms were computed with the following metrics:

- Accuracy: is the fraction of samples correctly classified
$$Accuracy = \frac{\textit{Number of correct predictions}}{\textit{Total number of predictions}} \tag{1}$$
- Recall: is the fraction of actual positive samples correctly identified
$$Recall = \frac{TP}{TP + FN} \tag{2}$$
where, TP = True Positive and FN = False Negative. In particular, we considered attack samples as positive and normal samples as negative.
- Precision: is the fraction of positive identifications correctly predicted.
$$Precision = \frac{TP}{TP + FP} \tag{3}$$
where, FP = False Positive.
- F1-score: is the harmonic mean of precision and recall.
$$Precision = \frac{2}{\frac{1}{precision} + \frac{1}{recall}} \tag{4}$$

D. EVALUATION RESULTS

Table 6 summarizes results in terms of Accuracy, Recall, Precision and F1-score for both physical and network datasets. Regarding the physical dataset, we obtained performance close to 100% for both RF and KNN; while NB and SVM returned lower performance for Precision and Recall.

On the other hand, machine learning applied to network dataset shows worse results. RF and KNN have better performance than those provided by SVM and NB; but, in all cases, the accuracy does not exceed 75%. Moreover, NB shows a poor ability to correctly detect true positive samples, as reported by the recall value which is less than 20%. On the contrary, SVM is prone to assign as anomalous the majority of samples, as reported by recall which is close to 100% and by precision which is just 10%.

Finally, we can conclude that machine learning algorithms singularly applied to network dataset are not sufficient in order to separate malicious and normal samples acquired from an ICS network. This behaviour is linked to the intrinsic inability of network data to report the current state of physical process which is essential in order to identify deviations from the correct dynamics. Thus, taking into account physical data from PLCs is necessary in order to properly recognize cyber attacks which have an impact against the physical process.

Moreover, as explained in Section III, our dataset provides some attack scenarios which have not any influence on network traffic, as in the case of physical attacks. During these scenarios, network data have not any information about the attack in progress resulting in the inability to recognize such attack.

On the other hand, we considered some cyber attacks, such as scanning attacks, which have effects only on network traffic. In these cases, physical data do not provide any discriminative features causing performance penalty.

Thus, in order to get better performance and in order to recognize all types of attacks, considering both network and physical data in the classification task is necessary.

VI. CONCLUSIONS

In this paper, we provided a new hardware-in-the-loop cyber-physical dataset obtained from a water distribution testbed.

The testbed is composed of a real subsystem and a simulated one, which was used in order to add complexity by increasing the number of tanks, valves, pumps and PLCs for the control. The dataset consists of both physical measurements and network traffic in order to overcome well-known limitations of the existing datasets by providing enough complexity and a more realistic network traffic with modern attack scenarios. Physical data was extracted by using a Historian machine, while network traffic was captured thanks to the *Wireshark* software. Such attacks were implemented in 28 different attack scenarios which consider both cyber and physical attacks. Their effects against physical and network dynamics can vary depending on the time, the attack type, the specific target and the current physical process. There are 41 features for the physical dataset and 14 features for the network one; in the latter, *Python* was used to extract and select features which best differentiate between normal and anomalous network packets.

Finally, we evaluated four machine learning algorithms, KNN, RF, NB and SVM, which were applied to both network and physical datasets. Results showed that classification algorithms cannot detect all the attacks types if they are applied separately on physical and network datasets. Thus, in order to get better performance, considering both network and physical data is necessary.

REFERENCES

[1] National Institute of Standards NIST and Technology. Information security. https://nvlpubs.nist.gov/nistpubs/Legacy/SP/nistspecialpublication800-39.pdf. Accessed: 2021-04-15.

[2] N. Jazdi. Cyber physical systems in the context of industry 4.0. In 2014 IEEE International Conference on Automation, Quality and Testing, Robotics, pages 1–4, 2014.

[3] M. M. Rana, L. Li, and S. W. Su. Cyber attack protection and control of microgrids. IEEE/CAA Journal of Automatica Sinica, 5(2):602–609, 2018.

[4] M. H. Cintuglu, O. A. Mohammed, K. Akkaya, and A. S. Uluagac. A survey on smart grid cyber-physical system testbeds. IEEE Communications Surveys Tutorials, 19(1):446–464, 2017.

[5] M. r. Akhondi, A. Talevski, S. Carlsen, and S. Petersen. Applications of wireless sensor networks in the oil, gas and resources industries. In 2010 24th IEEE International Conference on Advanced Information Networking and Applications, pages 941–948, 2010.

[6] Joe Weiss. Industrial Control System (ICS) Cyber Security for Water and Wastewater Systems, pages 87–105. 10 2014.

[7] KASPERSKY ICS CERT. Threat landscape for industrial automation systems. 2019.

[8] Chih-Che Sun, Adam Hahn, and Chen-Ching Liu. Cyber security of a power grid: State-of-the-art. International Journal of Electrical Power Energy Systems, 99:45–56, 07 2018.

[9] Hannes Holm, Martin Karresand, Arne Vidström, and Erik Westring. A survey of industrial control system testbeds. In Sonja Buchegger and Mads Dam, editors, Secure IT Systems, pages 11–26, Cham, 2015. Springer International Publishing.

[10] Qais Qassim, Norziana Jamil, Izham Zainal Abidin, Mohd Rusli, Salman Yussof, Roslan Ismail, Fairuz Abdullah, Norhamadi afar, Hafizah Hasan, and Maslina Daud. A survey of scada testbed implementation approaches. Indian Journal of Science and Technology, 10, 07 2017.

[11] Jonathan Goh, Sridhar Adepu, Khurum Junejo, and Aditya Mathur. A dataset to support research in the design of secure water treatment systems. pages 88–99, 11 2017.

[12] Pedro Laso, David Brosset, and John Puentes. Dataset of anomalies and malicious acts in a cyber-physical subsystem. Data in Brief, 14, 07 2017.

[13] Derui Ding, Qing-Long Han, Yang Xiang, Xiaohua Ge, and Xian-Ming Zhang. A survey on security control and attack detection for industrial cyber-physical systems. Neurocomputing, 275:1674–1683, 2018.

[14] S. Ghosh and S. Sampalli. A survey of security in scada networks: Current issues and future challenges. IEEE Access, 7:135812–135831, 2019.

[15] Kunal and M. Dua. Machine learning approach to ids: A comprehensive review. In 2019 3rd International conference on Electronics, Communication and Aerospace Technology (ICECA), pages 117–121, 2019.

[16] M. Almseidin, M. Alzubi, S. Kovacs, and M. Alkasassbeh. Evaluation of machine learning algorithms for intrusion detection system. In 2017 IEEE 15th International Symposium on Intelligent Systems and Informatics (SISY), pages 000277–000282, 2017.

[17] R. Vinayakumar, M. Alazab, K. P. Soman, P. Poornachandran, A. Al-Nemrat, and S. Venkatraman. Deep learning approach for intelligent intrusion detection system. IEEE Access, 7:41525–41550, 2019.

[18] A. S. Duque, S. Kanoor, D. Fraunholz, and H. S.Dieter. Evaluation of machine learning-based anomaly detection algorithms on an industrial modbus/tcp data set. In Proceedings of the 13th International Conference on Availability, Reliability and Security, ARES 2018, New York, NY, USA, 2018. Association for Computing Machinery.

[19] A. Özgür and H. Erdem. A review of kdd99 dataset usage in intrusion detection and machine learning between 2010 and 2015. PeerJ Preprints 4:e1954v1, 2016.

[20] M. Tavallaee, E. Bagheri, W. Lu, and A. A. Ghorbani. A detailed analysis of the kdd cup 99 data set. In 2009 IEEE Symposium on Computational Intelligence for Security and Defense Applications, pages 1–6, 2009.

[21] N. Moustafa and J. Slay. Unsw-nb15: a comprehensive data set for network intrusion detection systems (unsw-nb15 network data set). In 2015 Military Communications and Information Systems Conference (MilCIS), pages 1–6, 2015.

[22] An empirical comparison of botnet detection methods. Computers Security, 45:100–123, 2014.

[23] E. Perkins. Operational technology security – focus on securing industrial control and automation systems. 2014. https://blogs.gartner.com/earl-perkins/2014/03/14/operational-technology-security-focus-on-securing-industrial-control-and-automation-systems/.

[24] Seungoh Choi, Jeong-Han Yun, and Sin-Kyu Kim. A comparison of ics datasets for security research based on attack paths. In Eric Luiijf, Inga Žutautaitė, and Bernhard M. Hämmerli, editors, Critical Information Infrastructures Security, pages 154–166, Cham, 2019. Springer International Publishing.

[25] B. Zhu, A. Joseph, and S. Sastry. A taxonomy of cyber attacks on scada systems. In 2011 International Conference on Internet of Things and 4th International Conference on Cyber, Physical and Social Computing, pages 380–388, 2011.

[26] L. Cazorla, C. Alcaraz, and J. Lopez. Cyber stealth attacks in critical information infrastructures. IEEE Systems Journal, 12(2):1778–1792, 2018.

[27] Giuseppe Bernieri, Mauro Conti, and Federico Turrin. Evaluation of machine learning algorithms for anomaly detection in industrial networks. In 2019 IEEE International Symposium on Measurements Networking (M N), pages 1–6, 2019.

[28] Giuseppe Bernieri, Estefanía Etchevés Miciolino, Federica Pascucci, and Roberto Setola. Monitoring system reaction in cyber-physical testbed under cyber-attacks. Computers Electrical Engineering, 59:86–98, 2017.

[29] Daniele Antonioli and Nils Ole Tippenhauer. Minicps: A toolkit for security research on cps networks. In Proceedings of Workshop on Cyber-Physical Systems Security Privacy (SPC-CPS), co-located with CCS, October 2015.

[30] Joseph Prusa, Taghi M. Khoshgoftaar, and Naeem Seliya. The effect of dataset size on training tweet sentiment classifiers. In 2015 IEEE 14th International Conference on Machine Learning and Applications (ICMLA), pages 96–102, 2015.

[31] M. Endi, Y. Z. Elhalwagy, and A. hashad. Three-layer plc/scada system architecture in process automation and data monitoring. In 2010 The 2nd International Conference on Computer and Automation Engineering (ICCAE), volume 2, pages 774–779, 2010.

[32] Modicon modbus protocol reference guide, pi–mbus–300 rev. j. https://modbus.org/docs/PI_MBUS_300.pdf. Accessed: 2021-03-16.

[33] M. Mantere, I. Uusitalo, M. Sailio, and S. Noponen. Challenges of machine learning based monitoring for industrial control system networks. In 2012 26th International Conference on Advanced Information Networking and Applications Workshops, pages 968–972, 2012.

[34] Matti Mantere, Mirko Sailio, and Sami Noponen. Network traffic features for anomaly detection in specific industrial control system network. Future Internet, 5(4):460–473, 2013.
[35] Prasanta Gogoi, Monowar H. Bhuyan, D. K. Bhattacharyya, and J. K. Kalita. Packet and flow based network intrusion dataset. In Manish Parashar, Dinesh Kaushik, Omer F. Rana, Ravi Samtaney, Yuanyuan Yang, and Albert Zomaya, editors, Contemporary Computing, pages 322–334, Berlin, Heidelberg, 2012. Springer Berlin Heidelberg.
[36] A. Sperotto, G. Schaffrath, R. Sadre, C. Morariu, A. Pras, and B. Stiller. An overview of ip flow-based intrusion detection. IEEE Communications Surveys Tutorials, 12(3):343–356, 2010.
[37] Knn model-based approach in classification. Lecture Notes in Computer Science (including subseries Lecture Notes in Artificial Intelligence and Lecture Notes in Bioinformatics), 2888, 2003.
[38] Irina Rish. An empirical study of the naive bayes classifier. IJCAI 2001 workshop on empirical methods in artificial intelligence, 22230, 2001.
[39] William S. Noble. What is a support vector machine?, 2006.
[40] L Breiman. (impo)random forests(book). Machine learning, 2001.
[41] F. Pedregosa, G. Varoquaux, A. Gramfort, V. Michel, B. Thirion, O. Grisel, M. Blondel, P. Prettenhofer, R. Weiss, V. Dubourg, J. Vanderplas, A. Passos, D. Cournapeau, M. Brucher, M. Perrot, and E. Duchesnay. Scikit-learn: Machine learning in Python. Journal of Machine Learning Research, 12:2825–2830, 2011.

L. FARAMONDI received the Laurea degree in Computer Science and Automation (2013) and the PhD degree on Computer Science and Automation (2017) from the University RomaTre of Rome. He is currently assistant professor Fellow at Complex Systems & Security Laboratory at the University Campus Bio-Medico of Rome. He is involved in several national and European projects about the Critical Infrastructure and Indoor Localization. His research interests include the identification of network vulnerabilities, cyberphysical systems, and optimization at large. He is member of the IEEE SMC Technical Committee on Homeland Security (since 2017) and IEEE RAS Technical Committee on Digital Manufacturing and Human-Centered Automation (since 2020). He won the IEEE Systems, Man, and Cybernetics Society TCHS Young Researcher Award in 2021.

F. FLAMMINI (Senior Member, IEEE) was born in Formia, Italy, in 1978. He received the master's degree (cum laude) in computer engineering and the Ph.D. degree in computer and automation engineering from the University of Naples Federico II, Italy, in 2003 and 2006, respectively. From 2003 to 2016, he was a Software VV Engineer (2003-2007) and a Senior Innovation Engineer (2007-2016) with Ansaldo STS (now Hitachi Rail). From 2016 to 2017, he worked with the Italian State Mint and Polygraphic Institute as an Information Security Compliance Manager. Since 2018, he has been working as an Associate Professor with Linnaeus University, Sweden, where he has chaired the Cyber-Physical Systems (CPS) environment. Since 2020, he has also been a Professor of computer science with Mälardalen University, Sweden. He had leadership roles in more than ten research projects, has edited or authored more than ten books and 130 publications. His research interests include resilient cyber-physical systems and trustworthy autonomy. He is also an ACM Distinguished Speaker and the Chair of the IEEE SMC Technical Committee on Homeland Security.

S. GUARINO received the B.S. degree in received the cum laude Bachelor's degree in Industrial Engineering (2018) and the cum laude Master's degree in Biomedical Engineering (2020) with honor mention from the University Campus Bio-medico of Rome. He is currently PhD student at Complex Systems & Security Laboratory at the University Campus Bio-Medico of Rome. His scientific research focuses on prevention, identification, and mitigation of cyber-attacks against SCADA systems.

R. SETOLA (SM'07) received the Laurea degree in Electronic Engineering (1992) and the PhD in Control Engineering (1996) from the University of Naples "Federico II". He is Full Professor at the University Campus Bio-Medico, where he directs the Automation Research Unit and the Master Program in Homeland Security. He was responsible for the Italian Government Working Group on Critical Information Infrastructure Protection (CIIP) and a member of the G8 Senior Experts' group for CIIP. He has been the coordinator of several EU projects and he authored nine books and more than 250 scientific papers. His main research interests are the simulation, modeling and control of complex systems and Critical Infrastructure Protection.